Surface properties of neutron-rich exotic nuclei: A source for studying the nuclear symmetry energy

M.K. Gaidarov,[1] A.N. Antonov,[1] P. Sarriguren,[2] and E. Moya de Guerra[3]

[1]*Institute for Nuclear Research and Nuclear Energy, Bulgarian Academy of Sciences, Sofia 1784, Bulgaria*
[2]*Instituto de Estructura de la Materia, IEM-CSIC, Serrano 123, E-28006 Madrid, Spain*
[3]*Departamento de Fisica Atomica, Molecular y Nuclear, Facultad de Ciencias Fisicas, Universidad Complutense de Madrid, E-28040 Madrid, Spain*

We study the correlation between the thickness of the neutron skin in finite nuclei and the nuclear symmetry energy for isotopic chains of even-even Ni, Sn, and Pb nuclei in the framework of the deformed self-consistent mean-field Skyrme HF+BCS method. The symmetry energy, the neutron pressure and the asymmetric compressibility in finite nuclei are calculated within the coherent density fluctuation model using the symmetry energy as a function of density within the Brueckner energy-density functional. The mass dependence of the nuclear symmetry energy and the neutron skin thickness are also studied together with the role of the neutron-proton asymmetry. A correlation between the parameters of the equation of state (symmetry energy and its density slope) and the neutron skin is suggested in the isotopic chains of Ni, Sn, and Pb nuclei.

PACS numbers: 21.60.Jz, 21.65.Ef, 21.10.Gv

I. INTRODUCTION

The nuclear symmetry energy is a quantity of crucial importance in different areas of nuclear physics, including structure of ground-state nuclei [1–3], dynamics of heavy-ion reactions [4–6], physics of giant collective excitations [7] and physics of neutron stars [8–10]. Recently, the interest in the symmetry energy has been stirred up by novel astrophysical observations and by the availability of exotic beams in accelerators that provide additional information to the standard nuclear asymmetry studies based on stable nuclei. Particularly important in the different areas, and similarly uncertain, is the density dependence of the symmetry energy in uniform matter. As can be seen e.g., in Refs. [11–15], an increasing wide range of theoretical conclusions are being proposed on that density dependence, as well as on some associated nuclear characteristics. In the last years, the temperature dependence of single-particle properties in nuclear and neutron matter was also broadly investigated (e.g., Refs. [16, 17]).

Measurements of nuclear masses, densities, and collective excitations have allowed to resolve some of the basic features of the equation of state (EOS) of nuclear matter. However, the asymmetry properties of the EOS due to different neutron and proton numbers remain more elusive to date, and the study of the isospin dependent properties of asymmetric nuclear matter [18–22] and the density dependence of the nuclear symmetry energy remains a prime objective. The new radioactive ion beam facilities at CSR (China), FAIR (Germany), RIKEN (Japan), SPIRAL2/GANIL (France) and the upcoming FRIB (USA) will provide the possibility of exploring the properties of nuclear matter and nuclei under the extreme condition of large isospin asymmetry.

Experimentally, the symmetry energy is not a directly measurable quantity and has to be extracted indirectly from observables that are related to it (see, for example, the recent review [23]). The neutron skin thickness of nuclei is a sensitive probe of the nuclear symmetry energy, although its precise measurement is difficult to obtain. At present neutron skin thicknesses are derived from pygmy dipole resonances measurements [24], data from antiprotonic atoms [25] and other methods for its extraction like reactions and giant resonances. This allows one to constrain the parameters describing the nuclear symmetry energy.

Considering nuclei from the isotopic chains of Sn and Pb, Warda *et al.* [26] studied theoretically the bulk and the surface nature of the formation of the neutron skin, a concept that can be applied when analyzing the experimental data. The same authors indicated in Ref. [27] the role of the stiffness of the nuclear symmetry energy on the origin of the neutron skin thickness of ^{208}Pb, the latter being decomposed into bulk and surface components. Also, Danielewicz [28] has demonstrated that the ratio of the volume symmetry energy to the surface symmetry energy is closely related to the neutron skin thickness. The correlation between bulk and surface symmetry energy was further discussed in Refs. [8, 29–32]. Recent calculations of thermal nuclear properties showed that the surface symmetry energy term is more sensitive to temperature than the volume energy term [33].

The neutron skin thickness, generally defined as the difference between neutron and proton rms radii in the atomic nucleus, is closely correlated with the density dependence of the nuclear symmetry energy and with the equation of state of pure neutron matter. Moreover, it has been shown that the neutron skin thickness in heavy nuclei, like ^{208}Pb, calculated in mean-field models with either nonrelativistic or relativistic effective nuclear interactions, displays a linear correlation with the slope of the neutron EOS obtained with the same interactions at a neutron density $\rho \approx 0.10$ fm^{-3} [34, 35]. The statistical

analysis performed in Ref. [36] clearly shows the strong correlation that exists between the neutron form factor of ^{208}Pb and isovector indicators such as neutron skins and radii in neutron-rich nuclei, dipole polarizability, and nuclear matter properties (symmetry energy and pressure).

The symmetry energy of finite nuclei at saturation density is often extracted by fitting ground state masses with various versions of the liquid-drop mass (LDM) formula within liquid-drop models [37–39]. It has been also studied in the random phase approximation based on the Hartree-Fock (HF) approach [40] or effective relativistic Lagrangians with density-dependent meson-nucleon vertex functions [41], energy density functionals of Skyrme force [42–44] as well as relativistic nucleon-nucleon interaction [45, 46]. In the present work the symmetry energy will be studied *in a wide range of finite nuclei* on the basis of the Brueckner energy-density functional for nuclear matter [47, 48] and using the coherent density fluctuation model (CDFM) (e.g., Refs. [49, 50]). The latter is a natural extension of the Fermi gas model based on the generator coordinate method [50, 51] and includes long-range correlations of collective type. The CDFM has been applied to calculate the energies, the density distributions and rms radii of the ground and first monopole states in ^{4}He, ^{16}O and ^{40}Ca nuclei [52]. An analysis of breathing monopole states whose description is related mainly to general characteristics of atomic nuclei and weakly to the peculiarities of nuclear structure in the framework of the CDFM has been performed and also results for the incompressibility of finite nuclei have been reported [50, 53]. In Refs. [54, 55] the CDFM has been employed to calculate the scaling function in nuclei using the relativistic Fermi gas scaling function and the result has been applied to lepton scattering processes [54–60]. The CDFM analyses became useful to obtain information about the role of the nucleon momentum and density distributions for the explanation of superscaling in lepton-nucleus scattering [55, 56]. The CDFM scaling function has been used to predict cross sections for several processes: inclusive electron scattering in the quasielastic and Δ regions [57, 58] and neutrino (antineutrino) scattering both for charge-changing [58, 60] and for neutral-current [59, 60] processes. Recently, the CDFM was applied to study the scaling function and its connection with the spectral function and the momentum distribution [61].

In our previous study [62], we analyzed within a deformed HF+BCS approach with Skyrme-type density-dependent effective interactions the existence of a skin in nuclei far from the stability line by testing various definitions previously proposed [63, 64]. We have found that the neutron skin determined by the difference between neutron and proton radii using diffraction parameters defined in the Helm model [63] exhibits a more smooth, gradual increase with the neutron excess than the one obtained by means of definition from Ref. [64]. As a result, the absolute size of the skin ranges from 0.4 fm when the Helm model is used up to almost 1 fm for the heaviest isotopes using the criteria from Ref. [64]. The same Helm model definitions of the neutron skin thickness were studied in Ref. [65] in spherical self-consistent Hartree-Fock-Bogoliubov (HFB) calculations with finite-range Gogny forces. We would like to emphasize the consistency of the results of both approaches for the case of Ni and Sn isotopes [62, 65]. Some particular investigations of the neutron skin thickness of neutron-rich nuclei and its connections with the symmetry energy have been performed in the droplet model with surface width dependence [66] and in studies based on the Landau-Migdal approximation [67].

In the present work we investigate the relation between the neutron skin thickness and some nuclear matter properties in finite nuclei, such as the symmetry energy at the saturation point, symmetry pressure (proportional to the slope of the bulk symmetry energy), and asymmetric compressibility, considering nuclei in given isotopic chains and within a certain theoretical approach. In addition to various linear relations between several quantities in bulk matter and for a given nucleus that have been observed and tested within different theoretical methods (e.g. nonrelativistic calculations with different Skyrme parameter sets and relativistic models), we are looking forward to establish a possible correlation between the skin thickness and these quantities and to clarify to what extent this correlation is appropriate for a given isotopic chain. As in our previous papers [62, 68], we choose some medium and heavy Ni and Sn isotopes, because, first, they are primary candidates to be measured at the upcoming experimental facilities, and second, for them several predictions have been made concerning the nuclear skin emergence. In addition, we present some results for a chain of Pb isotopes being inspired by the significant interest (in both experiment [69] and theory [70]) to study, in particular, the neutron distribution of ^{208}Pb and its rms radius. The densities of these nuclei were calculated within a deformed HF+BCS approach with Skyrme-type density-dependent effective interactions [71, 72]. The results obtained in Ref. [62] demonstrated the ability of our microscopic theoretical method to predict the nuclear skin in exotic nuclei. As already mentioned, for a link between nuclear matter and finite nuclei we adopt the energy-density functional of Brueckner *et al.* [47, 48] that has been able to reproduce the binding energies and rms radii of light, medium, and heavy nuclei. The intrinsic properties of these nuclei are finally calculated in the CDFM framework that provides *an extension to realistic finite nuclear systems*. The evolution of the symmetry energy as we increase the number of neutrons is also studied. Additionally to Ref. [62], we pay more attention to the role of the neutron-proton asymmetry on the neutron skin formation.

The structure of this article is the following. In Sec. II we present the common definitions of symmetry energy and properties of nuclear matter which characterize its density dependence around normal nuclear matter density. Section III contains the CDFM formalism that provides a way to calculate the intrinsic quantities in finite

nuclei. There we give also the basic expressions for the model density distributions and nuclear radii obtained in the deformed HF+BCS method. The numerical results and discussions are presented in Sec. IV. We draw the main conclusions of this study in Sec. V.

II. THE KEY EOS PARAMETERS IN NUCLEAR MATTER

The symmetry energy $S(\rho)$ is defined by a Taylor series expansion of the energy per particle for nuclear matter (NM) in terms of the isospin asymmetry $\delta = (\rho_n - \rho_p)/\rho$

$$E(\rho,\delta) = E(\rho,0) + S(\rho)\delta^2 + O(\delta^4) + \cdots \ , \qquad (1)$$

where $\rho = \rho_n + \rho_p$ is the baryon density with ρ_n and ρ_p denoting the neutron and proton densities, respectively (see, e.g. [67, 73]). Odd powers of δ are forbidden by the isospin symmetry and the terms proportional to δ^4 and higher orders are found to be negligible.

Near the saturation density ρ_0 the energy of isospin-symmetric matter, $E(\rho,0)$, and the symmetry energy, $S(\rho)$, can be expanded as

$$E(\rho,0) = E_0 + \frac{K}{18\rho_0^2}(\rho-\rho_0)^2 + \cdots \ , \qquad (2)$$

and

$$\begin{aligned} S(\rho) &= \frac{1}{2}\left.\frac{\partial^2 E(\rho,\delta)}{\partial\delta^2}\right|_{\delta=0} \\ &= a_4 + \frac{p_0}{\rho_0^2}(\rho-\rho_0) + \frac{\Delta K}{18\rho_0^2}(\rho-\rho_0)^2 + \cdots \ . \end{aligned} \qquad (3)$$

The parameter a_4 is the symmetry energy at equilibrium ($\rho = \rho_0$). The pressure p_0^{NM}

$$p_0^{NM} = \rho_0^2 \left.\frac{\partial S}{\partial\rho}\right|_{\rho=\rho_0} \qquad (4)$$

and the curvature ΔK^{NM}

$$\Delta K^{NM} = 9\rho_0^2 \left.\frac{\partial^2 S}{\partial\rho^2}\right|_{\rho=\rho_0} \qquad (5)$$

of the nuclear symmetry energy at ρ_0 govern its density dependence and thus provide important information on the properties of the nuclear symmetry energy at both high and low densities. The widely used "slope" parameter L^{NM} is related to the pressure p_0^{NM} [Eq. (4)] by

$$L^{NM} = \frac{3p_0^{NM}}{\rho_0}. \qquad (6)$$

We remark that our present knowledge of these basic properties of the symmetry term around saturation is still very poor (see the analysis in Ref. [74] and references therein). In particular we note the uncertainty of the symmetry pressure at ρ_0 (sometimes it can vary by a factor of three) which is important for structure calculations. In practice, predictions for the symmetry energy vary substantially: *e.g.*, $a_4 \equiv S(\rho_0) = 28 - 38$ MeV. An empirical value of $a_4 \approx 29$ MeV has been extracted with reasonable accuracy from finite nuclei by fitting ground-state energies using the generalized Weizsäcker mass formula [29]:

$$\begin{aligned} E(N,Z) &= E_{mac} + E_{mic} \\ &= E_V + E_S + E_a + E_C + E_{mic} \\ &= -a_V A + a_S A^{2/3} + a_a\frac{(N-Z)^2}{A} \\ &+ a_C\frac{Z^2}{A^{1/3}} + E_{mic}, \end{aligned} \qquad (7)$$

where N and Z are the neutron and proton numbers, respectively, and $A = N+Z$ is the mass number. In Eq. (7) a_V, a_S, a_a and a_C are the volume, surface, symmetry and Coulomb coefficients. The microscopic energy E_{mic} contains shell- and pairing-energy corrections. It is worth to mention that the volume component of the symmetry energy coefficient a_a (or volume-symmetry coefficient in the empirical mass formula (7)) has to be attributed to the parameter a_4 in Eq. (3).

III. SYMMETRY ENERGY PARAMETERS OF FINITE NUCLEI IN CDFM

The CDFM was suggested and developed in Refs. [49, 50]. The model is related to the delta-function limit of the generator coordinate method [50, 51]. It is shown in the model that the one-body density matrix of the nucleus $\rho(\mathbf{r},\mathbf{r}')$ can be written as a coherent superposition of the one-body density matrices (OBDM) for spherical "pieces" of nuclear matter (so-called "fluctons") with densities

$$\rho_x(\mathbf{r}) = \rho_0(x)\Theta(x - |\mathbf{r}|), \qquad (8)$$

where

$$\rho_0(x) = \frac{3A}{4\pi x^3}. \qquad (9)$$

The generator coordinate x is the radius of a sphere containing Fermi gas of all A nucleons uniformly distributed in it. It is appropriate to use for such a system OBDM of the form:

$$\begin{aligned} \rho_x(\mathbf{r},\mathbf{r}') &= 3\rho_0(x)\frac{j_1(k_F(x)|\mathbf{r}-\mathbf{r}'|)}{(k_F(x)|\mathbf{r}-\mathbf{r}'|)} \\ &\times \ \Theta\left(x - \frac{|\mathbf{r}+\mathbf{r}'|}{2}\right), \end{aligned} \qquad (10)$$

where j_1 is the first-order spherical Bessel function and

$$k_F(x) = \left(\frac{3\pi^2}{2}\rho_0(x)\right)^{1/3} \equiv \frac{\alpha}{x} \qquad (11)$$

with

$$\alpha = \left(\frac{9\pi A}{8}\right)^{1/3} \simeq 1.52A^{1/3} \quad (12)$$

is the Fermi momentum of such a formation. Then the OBDM for the finite nuclear system can be written as a superposition of the OBDM's from Eq. (10):

$$\rho(\mathbf{r},\mathbf{r}') = \int_0^\infty dx|\mathcal{F}(x)|^2\rho_x(\mathbf{r},\mathbf{r}'). \quad (13)$$

In the CDFM the Wigner distribution function which corresponds to the OBDM from Eq. (13) is:

$$W(\mathbf{r},\mathbf{k}) = \int_0^\infty dx|\mathcal{F}(x)|^2 W_x(\mathbf{r},\mathbf{k}), \quad (14)$$

where

$$W_x(\mathbf{r},\mathbf{k}) = \frac{4}{(2\pi)^3}\Theta(x-|\mathbf{r}|)\Theta(k_F(x)-|\mathbf{k}|). \quad (15)$$

Correspondingly to $W(\mathbf{r},\mathbf{k})$ from Eq. (14), the density $\rho(\mathbf{r})$ in the CDFM is expressed by means of the same weight function $|\mathcal{F}(x)|^2$:

$$\begin{aligned}\rho(\mathbf{r}) &= \int d\mathbf{k} W(\mathbf{r},\mathbf{k}) \\ &= \int_0^\infty dx|\mathcal{F}(x)|^2\frac{3A}{4\pi x^3}\Theta(x-|\mathbf{r}|) \end{aligned} \quad (16)$$

normalized to the mass number:

$$\int \rho(\mathbf{r})d\mathbf{r} = A. \quad (17)$$

If one takes the delta-function approximation to the Hill-Wheeler integral equation in the generator coordinate method one gets a differential equation for the weight function $\mathcal{F}(x)$ [50, 51]. Instead of solving this differential equation we adopt a convenient approach to the weight function $|\mathcal{F}(x)|^2$ proposed in Refs. [49, 50]. In the case of monotonically decreasing local densities (*i.e.* for $d\rho(r)/dr \leq 0$), the latter can be obtained by means of a known density distribution $\rho(r)$ for a given nucleus [from Eq. (16)]:

$$|\mathcal{F}(x)|^2 = -\frac{1}{\rho_0(x)}\left.\frac{d\rho(r)}{dr}\right|_{r=x}. \quad (18)$$

The normalization of the weight function is:

$$\int_0^\infty dx|\mathcal{F}(x)|^2 = 1. \quad (19)$$

Considering the pieces of nuclear matter with density $\rho_0(x)$ (9) one can use for the matrix element $V(x)$ of the nuclear Hamiltonian the corresponding nuclear matter energy from the method of Brueckner *et al.* [47, 48]. In this energy-density method the expression for $V(x)$ reads

$$V(x) = AV_0(x) + V_C - V_{CO}, \quad (20)$$

where

$$\begin{aligned}V_0(x) &= 37.53[(1+\delta)^{5/3}+(1-\delta)^{5/3}]\rho_0^{2/3}(x) \\ &+ b_1\rho_0(x) + b_2\rho_0^{4/3}(x) + b_3\rho_0^{5/3}(x) \\ &+ \delta^2[b_4\rho_0(x) + b_5\rho_0^{4/3}(x) + b_6\rho_0^{5/3}(x)] \end{aligned} \quad (21)$$

with

$$\begin{aligned}b_1 &= -741.28, \quad b_2 = 1179.89, \quad b_3 = -467.54, \\ b_4 &= 148.26, \quad b_5 = 372.84, \quad b_6 = -769.57. \end{aligned} \quad (22)$$

$V_0(x)$ in Eq. (20) corresponds to the energy per nucleon in nuclear matter (in MeV) with the account for the neutron-proton asymmetry. V_C is the Coulomb energy of protons in a "flucton":

$$V_C = \frac{3}{5}\frac{Z^2e^2}{x} \quad (23)$$

and the Coulomb exchange energy is:

$$V_{CO} = 0.7386Ze^2(3Z/4\pi x^3)^{1/3}. \quad (24)$$

Thus, in the Brueckner EOS [Eq. (21)], the potential symmetry energy turns out to be proportional to δ^2. Only in the kinetic energy the dependence on δ is more complicated. Substituting $V_0(x)$ in Eq. (3) and taking the second derivative, the symmetry energy $S^{NM}(x)$ of the nuclear matter with density $\rho_0(x)$ (the coefficient a_4 in Eq. (3)) can be obtained:

$$\begin{aligned}S^{NM}(x) &= 41.7\rho_0^{2/3}(x) + b_4\rho_0(x) \\ &+ b_5\rho_0^{4/3}(x) + b_6\rho_0^{5/3}(x). \end{aligned} \quad (25)$$

The corresponding analytical expressions for the pressure $p_0^{NM}(x)$ and asymmetric compressibility $\Delta K^{NM}(x)$ of such a system in the Brueckner theory have the form:

$$\begin{aligned}p_0^{NM}(x) &= 27.8\rho_0^{5/3}(x) + b_4\rho_0^2(x) \\ &+ \frac{4}{3}b_5\rho_0^{7/3}(x) + \frac{5}{3}b_6\rho_0^{8/3}(x) \end{aligned} \quad (26)$$

and

$$\begin{aligned}\Delta K^{NM}(x) &= -83.4\rho_0^{2/3}(x) + 4b_5\rho_0^{4/3}(x) \\ &+ 10b_6\rho_0^{5/3}(x). \end{aligned} \quad (27)$$

Our basic assumption within the CDFM is that the symmetry energy, the slope and the curvature for finite nuclei can be defined weighting these quantities for nuclear matter (with a given density $\rho_0(x)$ (9)) by means of the weight function $|\mathcal{F}(x)|^2$. Thus, in the CDFM they will be an infinite superposition of the corresponding nuclear matter quantities. Following the CDFM scheme, the symmetry energy, the slope and the curvature have the following forms:

$$s = \int_0^\infty dx|\mathcal{F}(x)|^2 S^{NM}(x), \quad (28)$$

$$p_0 = \int_0^\infty dx |\mathcal{F}(x)|^2 p_0^{NM}(x), \tag{29}$$

$$\Delta K = \int_0^\infty dx |\mathcal{F}(x)|^2 \Delta K^{NM}(x). \tag{30}$$

We note that in the limit case when $\rho(r) = \rho_0 \Theta(R-r)$ (ρ_0 being the saturation density of symmetric nuclear matter) and $|\mathcal{F}(x)|^2$ becomes a delta-function (see Eq. (18)), Eq. (28) reduces to $S^{NM}(\rho_0) = a_4$.

The results that will be shown and discussed in the next section have been obtained from self-consistent deformed Hartree-Fock calculations with density-dependent Skyrme interactions [71] and accounting for pairing correlations. Pairing between like nucleons has been included by solving the BCS equations at each iteration with a fixed pairing strength that reproduces the odd-even experimental mass differences.

We consider in this paper the Skyrme SLy4 [75], Sk3 [76] and SG2 [77] parametrizations, namely because they are among the most extensively used Skyrme forces and have been already used in our previous paper [62]. In addition, we probe a recent LNS parameter set from Ref. [78], derived in the framework of the Brueckner-Hartree-Fock approximation that has been shown to work reasonably well for describing finite nuclei in the HF approximation.

The spin-independent proton and neutron densities are given by [62, 72]

$$\rho(\vec{R}) = \rho(r,z) = \sum_i 2 v_i^2 \rho_i(r,z)\,, \tag{31}$$

in terms of the occupation probabilities v_i^2 resulting from the BCS equations and the single-particle densities ρ_i

$$\rho_i(\vec{R}) = \rho_i(r,z) = |\Phi_i^+(r,z)|^2 + |\Phi_i^-(r,z)|^2\,, \tag{32}$$

with

$$\begin{aligned}\Phi_i^\pm(r,z) &= \frac{1}{\sqrt{2\pi}} \\ &\times \sum_\alpha \delta_{\Sigma,\pm 1/2}\, \delta_{\Lambda,\Lambda^\mp}\, C_\alpha^i\, \psi_{n_r}^\Lambda(r)\, \psi_{n_z}(z)\end{aligned} \tag{33}$$

and $\alpha = \{n_r, n_z, \Lambda, \Sigma\}$. The functions $\psi_{n_r}^\Lambda(r)$ and $\psi_{n_z}(z)$ entering Eq. (33) are defined in terms of Laguerre and Hermite polynomials

$$\psi_{n_r}^\Lambda(r) = \sqrt{\frac{n_r}{(n_r+\Lambda)!}}\, \beta_\perp\, \sqrt{2}\, \eta^{\Lambda/2}\, e^{-\eta/2}\, L_{n_r}^\Lambda(\eta)\,, \tag{34}$$

$$\psi_{n_z}(z) = \sqrt{\frac{1}{\sqrt{\pi} 2^{n_z} n_z!}}\, \beta_z^{1/2}\, e^{-\xi^2/2}\, H_{n_z}(\xi)\,, \tag{35}$$

with

$$\begin{aligned}\beta_z = (m\omega_z/\hbar)^{1/2} \;\;,\quad \beta_\perp = (m\omega_\perp/\hbar)^{1/2}, \\ \xi = z\beta_z \;\;,\quad \eta = r^2\beta_\perp^2\,.\end{aligned} \tag{36}$$

The normalization of the densities is given by

$$\int \rho(\vec{R}) d\vec{R} = X, \tag{37}$$

with $X = Z$, N for protons and neutrons, respectively.

The mean square radii for protons and neutrons are defined as

$$< r_{\rm p,n}^2 >= \frac{\int R^2 \rho_{\rm p,n}(\vec{R}) d\vec{R}}{\int \rho_{\rm p,n}(\vec{R}) d\vec{R}}\,, \tag{38}$$

and the rms radii are given by

$$r_{\rm p,n} =< r_{\rm p,n}^2 >^{1/2}\;. \tag{39}$$

Then the neutron skin thickness is usually characterized by the difference of neutron and proton rms radii:

$$\Delta R =< r_{\rm n}^2 >^{1/2} - < r_{\rm p}^2 >^{1/2}\,. \tag{40}$$

IV. RESULTS AND DISCUSSION

As the main emphasis of the present study is to inspect the correlation of the neutron skin thickness ΔR of nuclei in a given isotopic chain with the s, p_0 and ΔK parameters extracted from the density dependence of the symmetry energy around saturation density, we show first in Fig. 1 the results for Ni isotopes. The symmetry energy, the pressure and the asymmetric compressibility are calculated within the CDFM according to Eqs. (28)-(30) by using the weight functions (18) calculated from the self-consistent densities in Eq. (31). The differences between the neutron and proton rms radii of these isotopes [Eq. (40)] are obtained from HF+BCS calculations using four different Skyrme forces, SLy4, SG2, Sk3 and LNS. It is seen from Fig. 1(a) that there exists an approximate linear correlation between ΔR and s for the even-even Ni isotopes with $A = 74 - 84$. We observe a smooth growth of the symmetry energy till the double-magic nucleus ^{78}Ni ($N = 50$) and then a linear decrease of s while the neutron skin thickness of the isotopes increases. This behavior is valid for all Skyrme parametrizations used in the calculations, in particular, the average slope of ΔR for various forces is almost the same. The LNS force yields larger values of s comparing to the other three Skyrme interactions. In this case the small deviation can be attributed to the fact that the LNS force has not been fitted to finite nuclei and therefore, one cannot expect a good quantitative description at the same level as purely phenomenological Skyrme forces [78]. As a consequence, the neutron skin thickness calculated with LNS force has larger size with respect to the other three forces whose results for ΔR are comparable with each other. Nevertheless, it is worth to compare its predictions not only for ground-state nuclear properties but also for EOS characteristics of finite systems with those of other commonly used Skyrme forces.

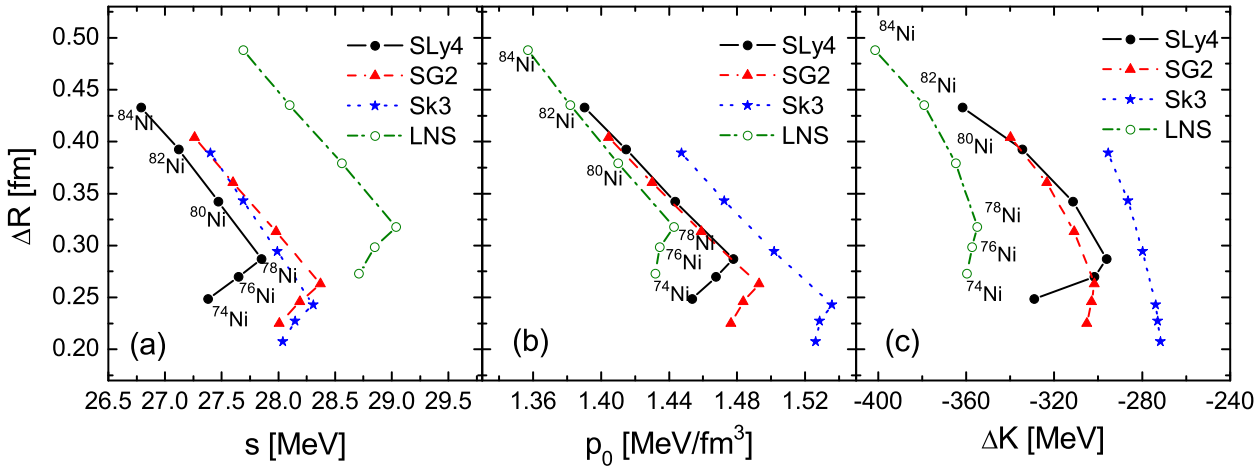

FIG. 1: (Color online) HF+BCS neutron skin thicknesses ΔR for Ni isotopes as a function of the symmetry energy s (a), pressure p_0 (b), and asymmetric compressibility ΔK (c) calculated with SLy4, SG2, Sk3, and LNS forces.

We also find a similar approximate linear correlation for Ni isotopes between ΔR and p_0 [Fig. 1(b)] and less strong correlation between ΔR and ΔK [Fig. 1(c)]. As in the symmetry energy case, the behavior of the curves drawn in these plots shows the same tendency, namely the inflexion point transition at the double-magic ^{78}Ni nucleus. We would like to note that the predictions for the difference ΔR between the rms radii of neutrons and protons with Skyrme forces obtained in Ref. [62] exhibited a steep change at the same place in which the number of neutrons starts to increase in the chain of nickel isotopes. In addition, the calculated results for the two-neutron separation energies and neutron and matter rms radii of the even Ni isotopes obtained in the relativistic Hartree-Bogoliubov framework [79] showed a quite strong kink at $N = 50$. Also one can see from Figs. 1(b) and 1(c) that the calculated values for p_0 and ΔK are lower in the case of LNS force than for the other three Skyrme parameter sets.

The results presented in Fig. 1(a) are illustrated in more details in Fig. 2, where the evolution of both neutron skin thickness and symmetry energy for Ni isotopes calculated with SLy4 force is given simultaneously on the same figure. For this chain our predictions for ΔR are extended to more neutron-rich isotopes ($A = 84$) comparing to the range of isotopes considered in Ref. [62]. The results for the symmetry energy obtained from the four different Skyrme parametrizations are compared in Fig. 3. It is seen that the trend of s when the mass number increases is preserved for all Skyrme forces but its values vary being very similar for SG2 and Sk3 forces. However, the magnitude of the symmetry energy values slowly changes and turns out to be approximately in the range of 27-29 MeV. The nuclear matter calculations relying on realistic nucleon-nucleon interactions appear to yield volume symmetry energy values within the same range of 27-29 MeV depending on the interaction [80].

As is known, radioactive ion beams enable us to study

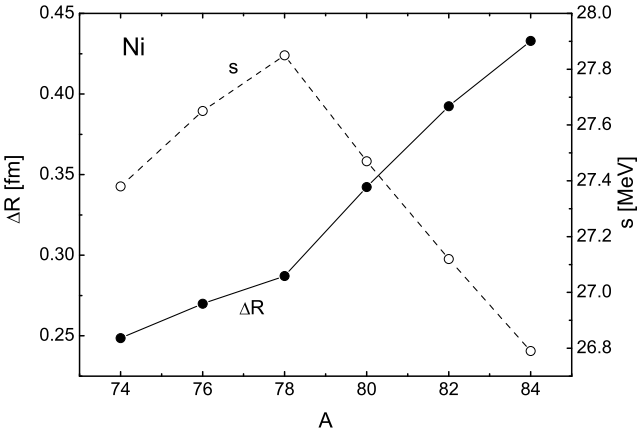

FIG. 2: HF+BCS neutron skin thicknesses ΔR (solid line) and symmetry energies s (dashed line) for Ni isotopes calculated with SLy4 force.

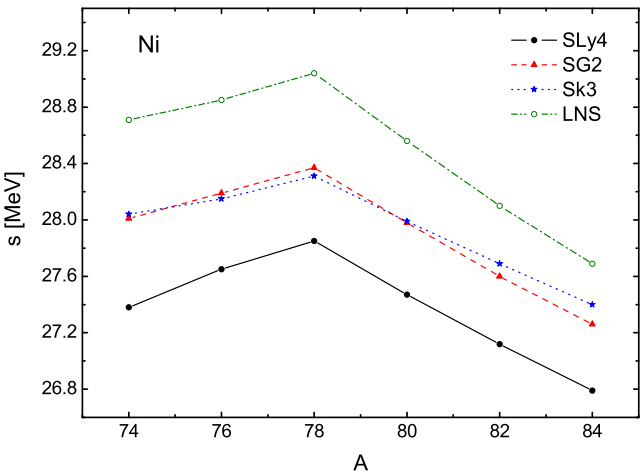

FIG. 3: (Color online) The symmetry energies s for Ni isotopes calculated with SLy4, SG2, Sk3, and LNS forces.

radii of unstable nuclei over a wide range of the relative neutron excess (or relative neutron-proton asymmetry) $I = (N-Z)/A$. The role of the global asymmetry on the neutron skin thickness in the Ni isotopic chain is shown in Fig. 4 for the case of SLy4 force by presenting results for the ratio $\Delta R/I$ as a function of the mass number A. It can be seen from Fig. 4 that due to the gradual increase of the skin thickness almost no dependence on I is observed for isotopes with $A < 78$, while for the heavier ones the ratio $\Delta R/I$ starts to increase rapidly with A. The latter takes place namely in the region where a pronounced neutron skin in Ni isotopes can be expected. We also give in Fig. 4 estimations for this ratio using the extended LDM formula for the binding energy of the nucleus [28, 30] (with neglected Coulomb contribution):

$$\Delta R^{LDM} = \frac{A^2 R}{6NZ(1 + A^{1/3}/y_s)} I. \tag{41}$$

In Eq. (41) $y_s \equiv S_V/S_S$ is the ratio between the volume and surface symmetry energies and its value is taken to be $y_s = 1.7$ [30]. For R we use $R \approx r_0 A^{1/3}$ with $r_0 = 1.2$ fm. As pointed out by Danielewicz [28], Eq. (41) is valid for the difference of sharp-sphere radii, but it is generalized for the case of rms radii that must be used. This creates an additional Coulomb correction [28] preserving unchanged the relation between ΔR and I. We see that the difference between the neutron and proton radii is linear in the global asymmetry in the absence of the Coulomb contribution (which, in principle, cannot be neglected) and measures the symmetry coefficient ratio. Thus, Fig. 4 displays how much the mean-field results differ from the LDM ones following the general observation that the neutron skin depends roughly linearly on the asymmetry of the nucleus. Although the Coulomb effects result in a reduction of the neutron skin for $N > Z$ nuclei [28, 30], it is important to note the direct relation between the skin thickness ΔR and the symmetry energy parameters (S_V, S_S) given by Eq. (41).

In this aspect, here we would like to mention that the finite nucleus symmetry energy within the extended LDM (which accounts for the surface effects) is given by [28–30]

$$a_a(A) = \frac{S_V}{1 + y_s A^{-1/3}}. \tag{42}$$

If one takes the same realistic values of $S_V = 27$ MeV and $y_s = 1.7$ [30] which we use when dealing with Eq. (41), it turns out that the values of a_a are in the interval 19–21 MeV for the nuclei ranging between ^{78}Ni and ^{208}Pb. These values are significantly smaller than the symmetry energy values s derived in CDFM from Eq. (28). As far as one of the main goals of our work is to calculate the nuclear symmetry energy of finite nuclei and to look for its relationship with the neutron skin thickness in these nuclei from a given isotopic chain, we would like to emphasize that the results obtained by using Eq. (28) represent estimations of the symmetry energy for finite nuclei obtained on the basis of nuclear matter EOS. A way to estimate the symmetry energy in finite nuclei within the mean-field framework has been recently proposed in [81], where Samaddar *et al.* studied the density and excitation energy dependence of symmetry energy and symmetry free energy of hot nuclei by using the local density approximation.

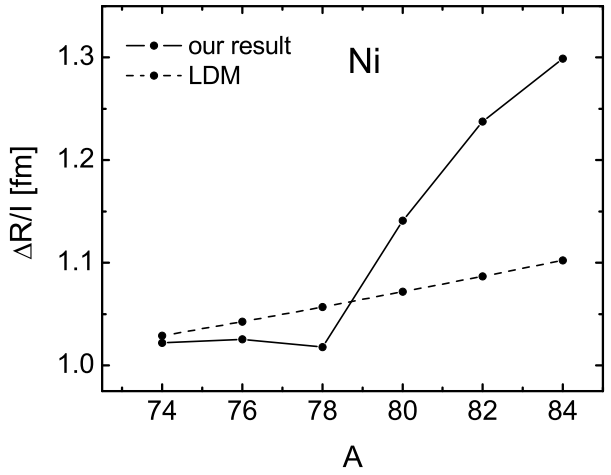

FIG. 4: The ratio $\Delta R/I$ for Ni isotopes calculated with SLy4 force (solid line) and obtained from Eq. (41) with LDM [28, 30] (dashed line).

In addition, it is important to note that by means of Eq. (28) we obtain the symmetry energy in finite nuclei including both bulk and surface contributions on the base of the Brueckner EOS. This is related to the usage in the method of the weight function $|\mathcal{F}(x)|^2$ which is computed by taking the derivative of the density distribution of a given finite nucleus [Eq. (18)]. Thus, information from both parts (central and surface) of the nuclear density is included in $|\mathcal{F}(x)|^2$ and, consequently, in the total symmetry energy. In this way, starting from the nuclear matter symmetry energy, we calculate by our method the total symmetry energy for the given finite nucleus. The use of different types of Skyrme effective forces leads to density distributions of protons and neutrons which slightly modify the weight function $|\mathcal{F}(x)|^2$. Increasing the number of neutrons at fixed proton number, Eq. (28) provides values for the symmetry energies s of considered isotopes that are found to change smoothly within a given chain.

As has been recently discussed (see, for instance, Refs. [28, 30, 32]), the relative contributions of the volume symmetry and surface symmetry energies can be disentangled using the extended LDM formula for the binding energy of the nucleus. A comparison between the symmetry energy values obtained in [32] (and listed in Table I of this reference) for SLy4 parametrization and those calculated in the present paper with the same force can be made. For example, the values of the total symmetry energy for the case of SLy4 extracted from leptodermous expansion in Ref. [82] and Eq. (42) vary between 19 and 23 MeV. Our values of the total sym-

metry energy (deduced with $|\mathcal{F}(x)|^2$ from calculations of the density corresponding to SLy4 force [Eq. (18)]) lie in the range of 26.8–27.8 MeV for Ni, 27.3–28.8 MeV for Sn, and 28.7–29.1 MeV for Pb isotopes. In our opinion, the differences of the compared results are due to the peculiarities of the two methods. As noted in the previous paragraph, in Eq. (28) we use $|\mathcal{F}(x)|^2$ obtained from both parts (central and surface) of the nuclear density, weighting by it the total symmetry energy for nuclear matter $S^{NM}(x)$. Second, in the present work $S^{NM}(x)$ is taken from the Brueckner theory, while in [32] (using the results of [82]) the *bulk* symmetry energy in the considered case of SLy4 parametrization is used. In principle, other functionals apart from the Brueckner one reported here can be applied within our method to calculate *the total symmetry energy for finite nuclei*, but as described above, the method gives it *unseparated into bulk and surface contributions*.

In Fig. 5 we display the theoretical neutron skin thickness ΔR of nuclei from a Pb isotopic chain against the parameters of interest s, p_0 and ΔK. Similarly to the three panels for Ni isotopes presented in Fig. 1, the predicted correlations manifest the same linear dependence. However, in this case the kink observed at double magic ^{208}Pb nucleus ($I \approx 0.21$) is much less pronounced that it can be seen at ^{78}Ni isotope ($I \approx 0.28$) and it does not change its direction. The value of ΔR for ^{208}Pb deduced from present HF+BCS calculations with SLy4 force is lower than the predicted thickness by the Skyrme Hartree-Fock model [42] and by the extended relativistic mean-field model [46], but fits well the values calculated with self-consistent densities of several nuclear mean-field models (see Table I in Ref. [27]). The p_0 and ΔK values for ^{208}Pb are in a good agreement with those from Ref. [42].

The analysis of the correlation between the neutron skin thickness and some macroscopic nuclear matter properties in finite nuclei is continued by showing the results for a chain of Sn isotopes. This is done in Fig. 6, where the results obtained with SLy4, SG2, Sk3, and LNS Skyrme forces are presented for isotopes with $A = 124 - 152$. Similarly to the case of Ni isotopes with transition at specific shell closure, we observe a smooth growth of the symmetry energy till the double-magic nucleus ^{132}Sn ($N = 82$) and then an almost linear decrease of s while the neutron skin thickness of the isotopes increases. In Ref. [62] we have studied a formation of a neutron skin in tin isotopes with smaller A where very poor experimental information is available. For instance, a large uncertainty is shown to exist experimentally in the neutron skin thickness of ^{124}Sn, i.e., its value varies from 0.1 to 0.3 fm depending on the experimental method. Our theoretical prediction $\Delta R = 0.17$ fm for this nucleus is found to be within the above experimental band. A similar approximate linear correlation between ΔR and p_0 for Sn isotopes is also shown in Fig. 6(b). Therefore, the neutron skin thickness of these nuclei can be extracted once the pressure p_0 at saturation density is known. The asymmetric compressibility ΔK given in Fig. 6(c) is less correlated than p_0 with ΔR within the Sn isotopic chains.

Figs. 7 and 8 illustrate the evolution of the symmetry energy with different Skyrme forces and the change of the neutron skin for Sn isotopes in SLy4 case. It is seen from Fig. 7 that the symmetry energies deduced from different Skyrme parametrizations vary in the interval 27-30 MeV. Similarly to the Ni isotopic chain (see Fig. 3), the LNS force yields values of s that overestimate the corresponding values of the other three Skyrme-type interactions. Also, the results for the symmetry energies calculated with both SG2 and Sk3 forces are comparable. At the same time the slope of all curves remains almost constant. As can be seen from Fig 8, the values of ΔR for ^{130}Sn and ^{132}Sn obtained from our HF+BCS calculations with SLy4 force fit very well the corresponding neutron skin thicknesses of 0.23 ± 0.04 fm and of 0.24 ± 0.04 fm of these nuclei derived from pygmy dipole resonances [24]. Moreover, both experimental and theoretical values follow a trend established by a measurement of the stable Sn isotopes [24, 62]. On the other hand, the extended region of Sn isotopes in the present study gives a good base for further measurements and systematic microscopic model calculations in order to assess the isospin dependence of the nuclear EOS.

In Fig. 9 is given the evolution of the ratio $\Delta R/I$ for Sn isotopes. A clear signal that a formation of a neutron skin can be expected to start at $A > 132$ is seen in favour of the magic nature of ^{132}Sn. Additionally, there is an indication for a weak shell closure at ^{140}Sn ($N = 88$). As in the case of Ni isotopes, the proportionality of the neutron skin thickness ΔR to the asymmetry parameter I following from the liquid-drop mass formula [Eq. (41)] leads to a gradual linear increase of $\Delta R/I$ with A also within the Sn isotopic chain. The corresponding numerical values of this ratio turn out to occupy some intermediate range comparing to our HF+BCS results.

The kinks displayed in Figs. 1-3 by the Ni isotopes and in Figs. 6-8 by the Sn isotopes can be attributed to the shell structure of these exotic nuclei. Indeed, the isotopic chains of Ni and Sn are of particular interest for nuclear structure calculations because of their proton shell closures at $Z = 28$ and $Z = 50$, respectively. They also extend from the proton drip line that is found nearby the double-magic ^{48}Ni (see, for instance, the discussion in Ref. [62] for a possible proton skin formation) and ^{100}Sn nuclei to the already β unstable neutron-rich double-magic ^{78}Ni and ^{132}Sn isotopes. In the case of ^{78}Ni ($N = 50$ shell closure) the filling of the $1g_{9/2}$ orbit is completed. Beyond this isotope the $2d_{5/2}$ subshell is being filled and a thick neutron skin is built up. Similar picture is present for the Sn isotopes. Here, one finds a sudden jump beyond $N = 82$ where the $1h_{11/2}$ shell is filled and the $2f_{7/2}$ subshell becomes populated. The situation in Pb isotopes shown in Fig. 5 is different from those of Ni and Sn isotopes-no kinks appear in the Pb chain considered. In the case of ^{208}Pb ($N = 126$) the $3p_{1/2}$ orbit is

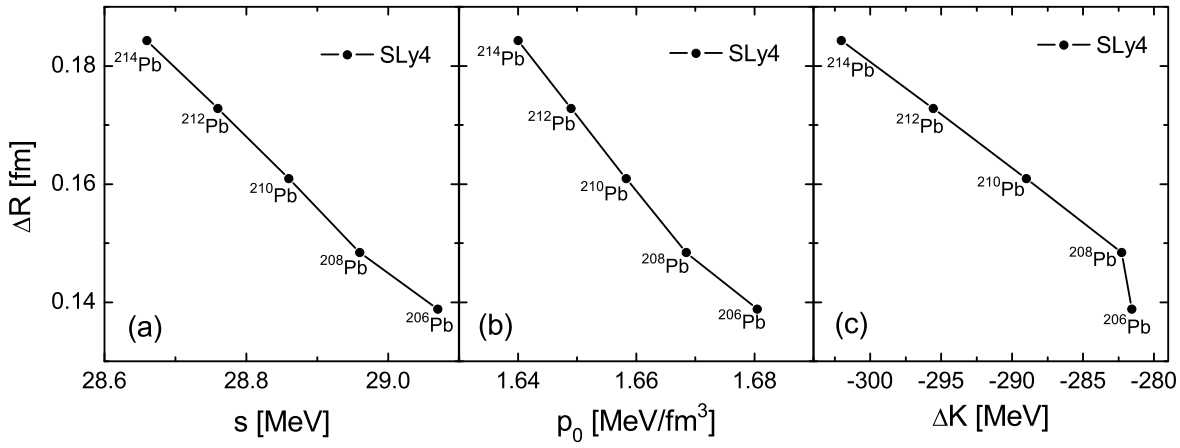

FIG. 5: HF+BCS neutron skin thicknesses ΔR for Pb isotopes as a function of the symmetry energy s (a), pressure p_0 (b), and asymmetric compressibility ΔK (c) calculated with SLy4 force.

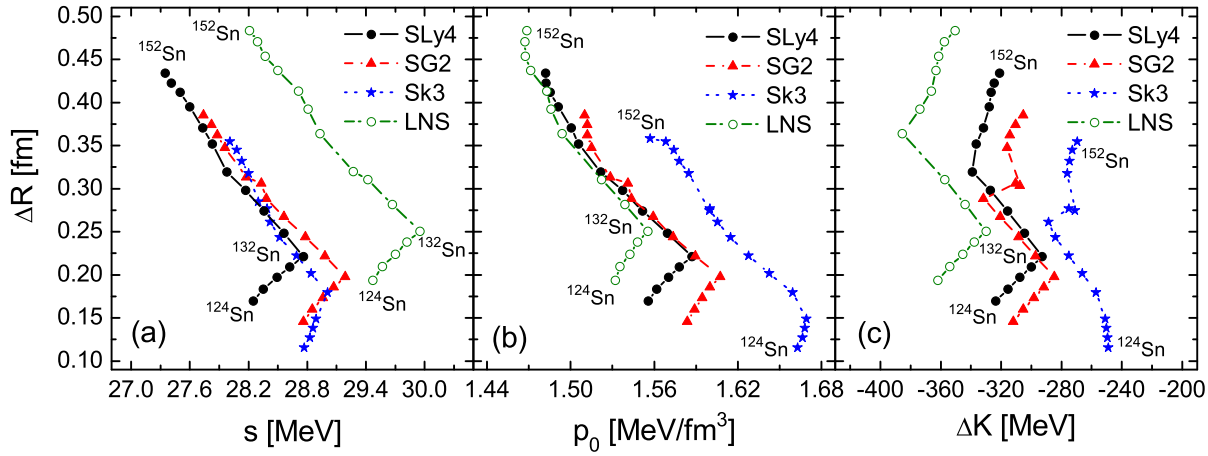

FIG. 6: (Color online) Same as in Fig. 1, but for Sn isotopes.

filled and above this nucleus the first occupied level is $2g_{9/2}$. As a result, the bulk and surface contributions to the neutron skin thickness of neutron-rich Sn and Pb isotopes reveal an opposite effect, namely the surface part dominates the bulk one in tins, while for Pb isotopes the bulk part is larger [26].

As it has been shown by Brown and Typel (see [34, 35]), and confirmed later by others [8, 25, 42, 67, 74], the neutron skin thickness (40) calculated in mean-field models with either nonrelativistic or relativistic effective interactions is very sensitive to the density dependence of the nuclear symmetry energy and, in particular, to the slope parameter L (respectively to the pressure p_0 [Eq. (6)]) at the normal nuclear saturation density. We note that while the basic idea behind studies of this type of correlations, namely between the neutron skin thickness and the symmetry energy (or the slope of the neutron EOS), is to constrain the symmetry energy in bulk matter from experimental results in finite nuclei, the main aim of our work is to extract quantitative information about s, p_0 and ΔK values for finite nuclei in CDFM. Moreover, so far in our work we presented another type of correlation, namely how these quantities are related to ΔR within a *given isotopic chain* apart from the same one for a *specific nucleus* using different theoretical models. Along this line we analyze the latter correlation and results for several Sn (^{132}Sn, ^{134}Sn, ^{156}Sn) isotopes and ^{78}Ni nucleus are shown in Fig. 10. Using the four sets of Skyrme interaction parameters, a linear fit to the correlation between ΔR and p_0 is performed to illustrate qualitatively the above correlation. It is seen from Figs. 10(a) and 10(d) that in the cases of double-magic ^{132}Sn and ^{78}Ni nuclei ΔR almost linearly correlates with p_0. If one goes from ^{132}Sn nucleus further to unstable nuclei within the same Sn isotopic chain the correlation becomes weaker, as it can be seen from Figs. 10(b) and 10(c), being almost the same in the case of neighbouring ^{134}Sn nucleus and poorly expressed in the case of far away ^{156}Sn isotope. Due to the limited number of Skyrme parametrizations used in our theo-

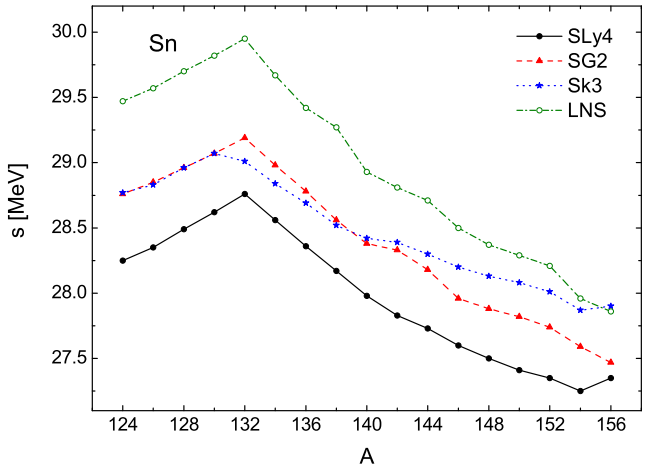

FIG. 7: (Color online) Same as in Fig. 3, but for Sn isotopes.

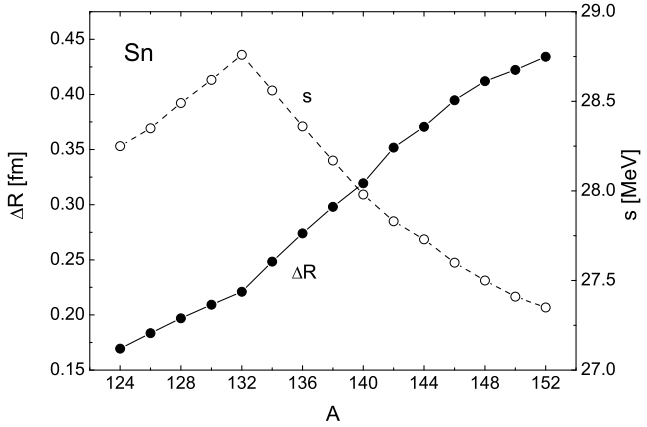

FIG. 8: Same as in Fig. 2, but for Sn isotopes.

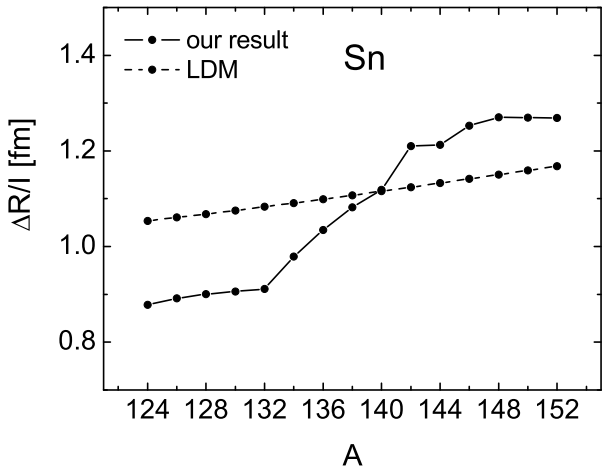

FIG. 9: Same as in Fig. 4, but for Sn isotopes.

retical approach, the results presented in Fig. 10 cannot provide a definite constraint of the slope (p_0 value) of the symmetry energy. Obviously, more complete confirmation of the existing correlation between the neutron skin thickness and the pressure for a given nucleus can be drawn when large set of nuclear models may be considered.

Finally, we would like to give estimations for the symmetry energy, pressure and incompressibility of asymmetric nuclear matter corresponding to the Brueckner EOS provided by the energy-density functional reported in Refs. [47, 48]. They are calculated at equilibrium density $\rho_0 = 0.204$ fm^{-3} for which the energy per nucleon V_0 [Eq. (21)] has a minimum. The latter ($E = -16.57$ MeV) is reached from the Brueckner formula at Fermi momentum $k_F = 1.446$ fm^{-1} and at the value of $\rho_0 = 0.204$ fm^{-3} used by us, as shown in Refs. [47, 83]. This value of ρ_0 is considered to be quite realistic [83]. The use of Eqs. (25)–(27) leads to the following estimations: $S^{NM} = 35.07$ MeV, $p_0^{NM} = 1.82$ MeV/fm^3, and $\Delta K^{NM} = -393.85$ MeV. It is seen that the symmetry energy is few MeV above the experimental range 28 MeV $\leq S^{NM} \leq$ 32 MeV [38] and the values deduced from our calculations for all finite nuclei considered. Also, the values of p_0^{NM} and ΔK^{NM} slightly overestimate the corresponding ones obtained in finite nuclei. Actually, the problem that the surface symmetry energy is very poorly constrained in the current energy density functional parametrizations, as well as by available phenomenological estimates, has been recently indicated in Ref. [32]. To illustrate this fact we would like to present here new symmetry energy values derived from the extended LDM. By taking $S_V = 35.07$ MeV which, however, comes out from the Brueckner EOS and a smaller value of $y_s = 1.1$ (corresponding to the fit with LDM formula in [30]), Eq. (42) gives values for the symmetry energy of 27.89 MeV for ^{78}Ni, 28.84 MeV for ^{132}Sn and 29.58 MeV for ^{208}Pb which are in a better agreement with the results obtained from Eq. (28). Studying relationships between the neutron skin and various properties of finite nuclei and infinite nuclear matter, it follows from the comparison that our microscopic theoretical approach produces results for these properties consistent with those provided by the Brueckner energy-density functional which may reduce the uncertainties of their future experimental extraction.

V. CONCLUSIONS

In this work, a theoretical approach to the nuclear many-body problem combining the deformed HF+BCS method with Skyrme-type density-dependent effective interactions [71] and the coherent density fluctuation model [49, 50] has been used to study nuclear properties of finite nuclei. For this purpose, we examined three chains of neutron-rich Ni, Sn, and Pb isotopes, most of them being far from the stability line and representing an interest for future measurements with radioactive exotic

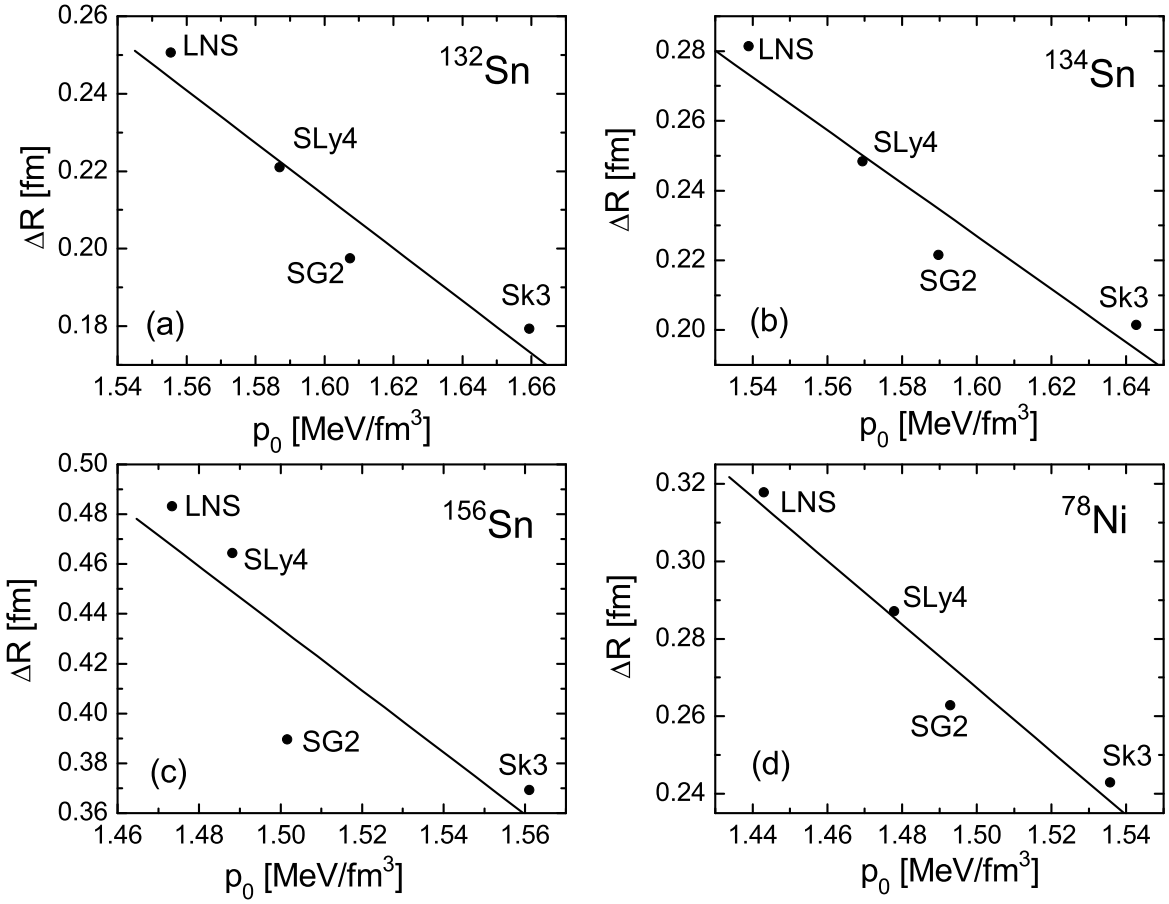

FIG. 10: HF+BCS neutron skin thicknesses ΔR for ^{132}Sn (a), ^{134}Sn (b), ^{156}Sn (c), and ^{78}Ni (d) as a function of the pressure p_0 for four sets of Skyrme interaction parameters: SLy4, SG2, Sk3, and LNS. The lines in all panels represent linear fits.

beams. Four Skyrme parametrizations were involved in the calculations: SG2, Sk3, SLy4, and LNS. In addition to the interactions used in Ref. [62], the LNS effective interaction was used in the present paper, because it has been built up from the EOS of nuclear matter including effects of three-body forces [78].

For the first time, we have demonstrated the capability of CDFM to be applied as an alternative way to make a transition *from the properties of nuclear matter to the properties of finite nuclei* investigating the nuclear symmetry energy s, the neutron pressure p_0 and the asymmetric compressibility ΔK in finite nuclei. This has been carried out on the base of the Brueckner energy-density functional for infinite nuclear matter. Mainly, the symmetry energy has been determined from analyzing nuclear masses within liquid-drop models, while much more effort has been recently devoted to extracting the value of its slope parameter. Instead of this, in the present work we applied the CDFM scheme. One of the advantages of the CDFM is the possibility to obtain transparent relations for the intrinsic EOS quantities analytically by means of a convenient approach to the weight function. The key element of this model is the choice of density distributions which were taken from self-consistent deformed HF+BCS calculations.

We would like to emphasize that our new method allows one to estimate the symmetry energy and, therefore, the symmetry-energy coefficient in finite nuclei thus avoiding the problems related to fitting the Hartree-Fock energies to a LDM parametrization.

We have found that there exists an approximate linear correlation between the neutron skin thickness of even-even nuclei from the Ni ($A = 74-84$), Sn ($A = 124-152$), and Pb ($A = 206-214$) isotopic chains and their nuclear symmetry energies. Our HF+BCS calculations lead to a symmetry energy in the range of 27-30 MeV, which is in agreement with the empirical value of 30 ± 4 MeV [84] and with the results of Nikolov *et al.* [32]. In the cases of Ni and Sn isotopes the symmetry energy is found to increase almost linearly with the mass number A till the double-magic nuclei (^{78}Ni and ^{132}Sn) and then to decrease, being larger when LNS force is used. A similar linear correlation between ΔR and p_0 is also found to exist, while the relation between ΔR and ΔK is less pronounced. The same behavior containing an inflexion point transition at specific shell closure is ob-

served for these correlations. The calculated values of $p_0 = 1.36 - 1.68$ MeV/fm^3 obtained in our calculations lead to values of the slope parameter $L = 26 - 32$ MeV that are in agreement with other theoretical predictions (see, for example [42]). Hence, the study of other two EOS parameters (whose determination is more uncertain than the symmetry energy), namely the slope and the curvature of s, performed in our work may provide more constraints on both the density dependence of the nuclear symmetry energy and the thickness of the neutron skin in neutron-rich medium and heavy nuclei.

In the present work, the role of the relative neutron-proton asymmetry I on the size of the neutron skin ΔR was studied for Ni and Sn isotopes. For this purpose the results for the ratio $\Delta R/I$ were presented and a comparison with its estimation using the extended liquid-drop mass formula [Eq. (41)] was made. The HF+BCS results show that a formation of a neutron skin can be expected to start at $A > 78$ and $A > 132$ for Ni and Sn isotopes, respectively. Although the proportionality that exists between ΔR and I in (41) produces smooth change of ΔR with A, the size of the neutron skin in both cases is consistent with the results of other calculations with the SLy4 parametrization [63], as well as with results of spherical self-consistent HFB calculations with finite-range forces of the Gogny type [65]. It is confirmed that the neutron skins in nuclei with a large neutron excess near and beyond the drip line are very clearly related to the asymmetry parameter I. However, the shell effects, which are always present in mean-field calculations, produce deviations from the linear dependence between ΔR and I in these nuclei.

Summarizing, in this work we use a microscopic theoretical approach to study important macroscopic nuclear matter quantities in finite nuclei and their relation to surface properties of neutron-rich exotic nuclei. We have shown that this approach gives a very reasonable description of the neutron skin thicknesses of several Sn isotopes which have been experimentally measured. A good agreement is achieved with other theoretical predictions for the volume symmetry energies of Ni isotopes, as well as for the pressure and asymmetric compressibility of nuclei within the Pb isotopic chain. The capability of the present method can be further demonstrated by taking into consideration Skyrme-type and relativistic nuclear energy-density functionals. In this way, more systematic analysis of the relationship between the symmetry energy and the neutron skin thickness will be carried out and more definite conclusions on its isotopic sensitivity will be drawn.

Acknowledgments

Two of the authors (M.K.G. and A.N.A.) are grateful for the support of the Bulgarian Science Fund under Contract No. 02–285. E.M.G. and P.S. acknowledge support from MICINN (Spain) under Contracts FIS2008–01301 and FPA2010–17142.

[1] T. Nikšić, D. Vretenar, and P. Ring, Phys. Rev. C **78**, 034318 (2008).
[2] N. Van Giai, B. V. Carlson, Z. Ma, and H. Wolter, J. Phys. G **37**, 064043 (2010).
[3] E. N. E. van Dalen and H. Müther, arXiv:1004.0144 [nucl-th] (2010).
[4] Bao-An Li, Lie-Wen Chen, and Che Ming Ko, Phys. Rep. **464**, 113 (2008).
[5] Lie-Wen Chen, Che Ming Ko, Bao-An Li, and Gao-Chan Yong, Int. J. Mod. Phys. E **17**, 1825 (2008).
[6] M. Colonna, J. Phys. Conf. Ser. **168**, 012006 (2009).
[7] V. Rodin, Prog. Part. Nucl. Phys. **59**, 268 (2007).
[8] A. W. Steiner, M. Prakash, J. M. Lattimer, and P. J. Ellis, Phys. Rep. **411**, 325 (2005).
[9] V. P. Psonis, Ch. C. Moustakidis, and S. E. Massen, Mod. Phys. Lett. A **22**, 1233 (2007).
[10] Bharat K. Sharma and Subrata Pal, Phys. Lett. B **682**, 23 (2009).
[11] Z. H. Li, U. Lombardo, H.-J. Schulze, W. Zuo, L. W. Chen, and H. R. Ma, Phys. Rev. C **74**, 047304 (2006).
[12] J. Piekarewicz and M. Centelles, Phys. Rev. C **79**, 054311 (2009).
[13] I. Vidaña, C. Providência, A. Polls, and A. Rios, Phys. Rev. C **80**, 045806 (2009).
[14] F. Sammarruca and P. Liu, Phys. Rev. C **79**, 057301 (2009).
[15] P. Danielewicz, arXiv:1003.4011 [nucl-th] (2010).
[16] Ch. C. Moustakidis, Phys. Rev. C **76**, 025805 (2007).
[17] F. Sammarruca, arXiv:0908.1958 [nucl-th] (2009).
[18] K. Oyamatsu, I. Tanihata, Y. Sugahara, K. Sumiyoshi, and H. Toki, Nucl. Phys. A **634**, 3 (1998).
[19] W. Zuo, I. Bombaci, and U. Lombardo, Phys. Rev. C **60**, 024605 (1999).
[20] P. Roy Chowdhury, D. N. Basu, and C. Samanta, Phys. Rev. C **80**, 011305(R) (2009).
[21] Lie-Wen Chen, Bao-Jun Cai, Che Ming Ko, Bao-An Li, Chun Shen, and Jun Xu, Phys. Rev. C **80**, 014322 (2009).
[22] P. Gögelein, E. N. E. van Dalen, Kh. Gad, S. A. Hassaneen, and H. Müther, Phys. Rev. C **79**, 024308 (2009).
[23] D. V. Shetty and S. J. Yennello, Pramana **75**, 259 (2010); arXiv:1002.0313 [nucl-ex] (2010).
[24] A. Klimkiewicz *et al.*, Phys. Rev. C **76**, 051603(R) (2007).
[25] M. Centelles, X. Roca-Maza, X. Viñas, and M. Warda, Phys. Rev. Lett. **102**, 122502 (2009).
[26] M. Warda, X. Viñas, X. Roca-Maza, and M. Centelles, Phys. Rev. C **81**, 054309 (2010).
[27] M. Centelles, X. Roca-Maza, X. Viñas, and M. Warda, Phys. Rev. C **82**, 054314 (2010).
[28] P. Danielewicz, Nucl. Phys. A **727**, 233 (2003).
[29] P. Danielewicz and J. Lee, AIP Conf. Proc. **947**, 301 (2007); Nucl. Phys. A **818**, 36 (2009).

[30] A. E. L. Dieperink and P. Van Isacker, Eur. Phys. J. A **32**, 11 (2007).

[31] V. M. Kolomietz and A. I. Sanzhur, Eur. Phys. J. A **38**, 345 (2008); Phys. Rev. C **81**, 024324 (2010).

[32] N. Nikolov, N. Schunck, W. Nazarewicz, M. Bender, and J. Pei, Phys. Rev. C **83**, 034305 (2011).

[33] S. J. Lee and A. Z. Mekjian, Phys. Rev. C **82**, 064319 (2010).

[34] B. Alex Brown, Phys. Rev. Lett. **85**, 5296 (2000).

[35] S. Typel and B. Alex Brown, Phys. Rev. C **64**, 027302 (2001).

[36] P.-G. Reinhard and W. Nazarewicz, Phys. Rev. C **81**, 051303(R) (2010).

[37] W. D. Myers and W. J. Swiatecki, Nucl. Phys. A **81**, 1 (1966).

[38] P. Möller *et al.*, At. Data Nucl. Data Tables **59**, 185 (1995).

[39] K. Pomorski and J. Dudek, Phys. Rev. C **67**, 044316 (2003).

[40] A. Carbone, G. Colò, A. Bracco, Li-Gang Cao, P. F. Bortignon, F. Camera, and O. Wieland, Phys. Rev. C **81**, 041301(R) (2010).

[41] D. Vretenar, T. Nikšić, and P. Ring, Phys. Rev. C **68**, 024310 (2003).

[42] Lie-Wen Chen, Che Ming Ko, and Bao-An Li, Phys. Rev. C **72**, 064309 (2005).

[43] Satoshi Yoshida and Hiroyuki Sagawa, Phys. Rev. C **73**, 044320 (2006).

[44] Lie-Wen Chen, Che Ming Ko, Bao-An Li, and Jun Xu, arXiv:1004.4672 [nucl-th] (2010).

[45] C.-H. Lee, T. T. S. Kuo, G. Q. Li, and G. E. Brown, Phys. Rev. C **57**, 3488 (1998).

[46] B. K. Agrawal, Phys. Rev. C **81**, 034323 (2010).

[47] K. A. Brueckner, J. R. Buchler, S. Jorna, and R. J. Lombard, Phys. Rev. **171**, 1188 (1968).

[48] K. A. Brueckner, J. R. Buchler, R. C. Clark, and R. J. Lombard, Phys. Rev. **181**, 1543 (1969).

[49] A. N. Antonov, V. A. Nikolaev, and I. Zh. Petkov, Bulg. J. Phys. **6**, 151 (1979); Z. Phys. A **297**, 257 (1980); *ibid* **304**, 239 (1982); Nuovo Cimento A **86**, 23 (1985); A. N. Antonov *et al.*, *ibid* **102**, 1701 (1989); A. N. Antonov, D. N. Kadrev, and P. E. Hodgson, Phys. Rev. C **50**, 164 (1994).

[50] A. N. Antonov, P. E. Hodgson, and I. Zh. Petkov, *Nucleon Momentum and Density Distributions in Nuclei* (Clarendon Press, Oxford, 1988); *Nucleon Correlations in Nuclei* (Springer-Verlag, Berlin-Heidelberg-New York, 1993).

[51] J. J. Griffin and J. A. Wheeler, Phys. Rev. **108**, 311 (1957).

[52] A. N. Antonov, I. S. Bonev, Chr. V. Christov, and I. Zh. Petkov, Nuovo Cimento A **100**, 779 (1988).

[53] A. N. Antonov, V. A. Nikolaev, and I. Zh. Petkov, Bulg. J. Phys. **18**, 107 (1991).

[54] A. N. Antonov, M. K. Gaidarov, D. N. Kadrev, M. V. Ivanov, E. Moya de Guerra, and J. M. Udias, Phys. Rev. C **69**, 044321 (2004).

[55] A. N. Antonov, M. K. Gaidarov, M. V. Ivanov, D. N. Kadrev, E. Moya de Guerra, P. Sarriguren, and J. M. Udias, Phys. Rev. C **71**, 014317 (2005).

[56] A. N. Antonov, M. V. Ivanov, M. K. Gaidarov, E. Moya de Guerra, P. Sarriguren, and J. M. Udias, Phys. Rev. C **73**, 047302 (2006).

[57] A. N. Antonov, M. V. Ivanov, M. K. Gaidarov, E. Moya de Guerra, J. A. Caballero, M. B. Barbaro, J. M. Udias, and P. Sarriguren, Phys. Rev. C **74**, 054603 (2006).

[58] M. V. Ivanov, M. B. Barbaro, J. A. Caballero, A. N. Antonov, E. Moya de Guerra, and M. K. Gaidarov, Phys. Rev. C **77**, 034612 (2008).

[59] A. N. Antonov, M. V. Ivanov, M. B. Barbaro, J. A. Caballero, E. Moya de Guerra, and M. K. Gaidarov, Phys. Rev. C **75**, 064617 (2007).

[60] A. N. Antonov, M. V. Ivanov, M. B. Barbaro, J. A. Caballero, and E. Moya de Guerra, Phys. Rev. C **79**, 044602 (2009).

[61] J. A. Caballero, M. B. Barbaro, A. N. Antonov, M. V. Ivanov, and T. W. Donnelly, Phys. Rev. C **81**, 055502 (2010).

[62] P. Sarriguren, M. K. Gaidarov, E. Moya de Guerra, and A. N. Antonov, Phys. Rev. C **76**, 044322 (2007).

[63] S. Mizutori, J. Dobaczewski, G. A. Lalazissis, W. Nazarewicz, and P.-G. Reinhard, Phys. Rev. C **61**, 044326 (2000).

[64] N. Fukunishi, T. Otsuka, and I. Tanihata, Phys. Rev. C **48**, 1648 (1993).

[65] N. Schunck and J. L. Egido, Phys. Rev. C **78**, 064305 (2008).

[66] M. Warda, X. Viñas, X. Roca-Maza, and M. Centelles, Phys. Rev. C **80**, 024316 (2009).

[67] A. E. L. Dieperink, Y. Dewulf, D. Van Neck, M. Waroquier, and V. Rodin, Phys. Rev. C **68**, 064307 (2003).

[68] A. N. Antonov, D. N. Kadrev, M. K. Gaidarov, E. Moya de Guerra, P. Sarriguren, J. M. Udias, V. K. Lukyanov, E. V. Zemlyanaya, and G. Z. Krumova, Phys. Rev. C **72**, 044307 (2005).

[69] http://hallaweb.jlab.org/parity/prex .

[70] O. Moreno, E. Moya de Guerra, P. Sarriguren, and J. M. Udias, J. Phys. G **37**, 064019 (2010).

[71] D. Vautherin, Phys. Rev. C **7**, 296 (1973).

[72] E. Moya de Guerra, P. Sarriguren, J. A. Caballero, M. Casas, and D. W. L. Sprung, Nucl. Phys. A **529**, 68 (1991).

[73] Lie-Wen Chen, Phys. Rev. C **83**, 044308 (2011).

[74] R. J. Furnstahl, Nucl. Phys. **A706**, 85 (2002).

[75] E. Chabanat, P. Bonche, P. Haensel, J. Meyer, and R. Schaeffer, Nucl. Phys. A **635**, 231 (1998).

[76] M. Beiner, H. Flocard, N. Van Giai, and P. Quentin, Nucl. Phys. A **238**, 29 (1975).

[77] N. Van Giai and H. Sagawa, Phys. Lett. B **106**, 379 (1981).

[78] L. G. Cao, U. Lombardo, C. W. Shen, and N. Van Giai, Phys. Rev. C **73**, 014313 (2006).

[79] J. Meng, Phys. Rev. C **57**, 1229 (1998).

[80] L. Engvik, M. Hjorth-Jensen, R. Machleidt, H. Müther, and A. Polls, Nucl. Phys. A **627**, 85 (1997).

[81] S. K. Samaddar, J. N. De, X. Viñas, and M. Centelles, Phys. Rev. C **76**, 041602(R) (2007); *ibid* **78**, 034607 (2008).

[82] P.-G. Reinhard, M. Bender, W. Nazarewicz, and T. Vertse, Phys. Rev. C **73**, 014309 (2006).

[83] H. A. Bethe, *Theory of Nuclear Matter*, Annual Review of Nuclear Science, vol. 21, (Palo Alto, California, USA, 1971), p.93.

[84] P. E. Haustein, At. Data Nucl. Data Tables **39**, 185 (1988).